Title

Mitochondrial Proton Leak Regulated by Cyclophilin D Elevates Insulin Secretion in Islets at Nonstimulatory Glucose Levels

Journal

Diabetes, 69(2)

ISSN

0012-1797

Authors

Taddeo, Evan P
Alsabeeh, Nour
Baghdasarian, Siyouneh
et al.

Publication Date

2020-02-01

DOI

10.2337/db19-0379

Peer reviewed

Mitochondrial Proton Leak Regulated by Cyclophilin D Elevates Insulin Secretion in Islets at Nonstimulatory Glucose Levels

Evan P. Taddeo,[1] Nour Alsabeeh,[1,2] Siyouneh Baghdasarian,[1] Jakob D. Wikstrom,[3] Eleni Ritou,[1] Samuel Sereda,[4] Karel Erion,[1] Jin Li,[1] Linsey Stiles,[1] Muhamad Abdulla,[5] Zachary Swanson,[5] Joshua J. Wilhelm,[5] Melena D. Bellin,[5,6] Richard G. Kibbey,[7] Marc Liesa,[1,8] and Orian S. Shirihai[1]

Diabetes 2020;69:131–145 | https://doi.org/10.2337/db19-0379

Fasting hyperinsulinemia precedes the development of type 2 diabetes. However, it is unclear whether fasting insulin hypersecretion is a primary driver of insulin resistance or a consequence of the progressive increase in fasting glycemia induced by insulin resistance in the prediabetic state. Herein, we have discovered a mechanism that specifically regulates non–glucose-stimulated insulin secretion (NGSIS) in pancreatic islets that is activated by nonesterified free fatty acids, the major fuel used by β-cells during fasting. We show that the mitochondrial permeability transition pore regulator cyclophilin D (CypD) promotes NGSIS, but not glucose-stimulated insulin secretion, by increasing mitochondrial proton leak. Islets from prediabetic obese mice show significantly higher CypD-dependent proton leak and NGSIS compared with lean mice. Proton leak–mediated NGSIS is conserved in human islets and is stimulated by exposure to nonesterified free fatty acids at concentrations observed in obese subjects. Mechanistically, proton leak activates islet NGSIS independently of mitochondrial ATP synthesis but ultimately requires closure of the K_{ATP} channel. In summary, we have described a novel nonesterified free fatty acid–stimulated pathway that selectively drives pancreatic islet NGSIS, which may be therapeutically exploited as an alternative way to halt fasting hyperinsulinemia and the progression of type 2 diabetes.

Type 2 diabetes ultimately manifests when islets fail to continue hypersecreting insulin to counteract insulin resistance. On the basis of this premise, it is commonly believed that hyperinsulinemia during the fasted state occurs solely as a compensatory response to fasting hyperglycemia induced by insulin resistance. However, high levels of insulin contribute more to insulin resistance than hyperglycemia (1), elevated fasting insulin precedes the development of severe fasting hyperglycemia (2–4), and fasting hyperinsulinemia is one of the most powerful predictors of type 2 diabetes development (5,6). Remarkably, isolated islets from insulin-resistant mice continue to hypersecrete insulin when cultured under very low glucose concentrations (7,8), but the underlying mechanisms are poorly understood. Moreover, mice with reduced capacity to produce insulin (9) or with reduced lipolysis in β-cells (10) are protected from obesity and insulin resistance induced by high-fat diet (HFD) feeding. Likewise, fasting hyperinsulinemia in patients with prediabetes may also be linked to enhanced use of nonesterified fatty acids

[1]Division of Endocrinology, Diabetes and Hypertension, Department of Medicine, David Geffen School of Medicine at UCLA, Los Angeles, CA
[2]Department of Physiology, Faculty of Medicine, Kuwait University, Kuwait City, Kuwait
[3]Dermatology and Venereology Unit, Department of Medicine, Karolinska Institutet, and Department of Dermato-Venereology, Karolinska University Hospital, Stockholm, Sweden
[4]Endocrinology, Diabetes, Nutrition and Weight Management Section, Department of Medicine, Boston University School of Medicine, Boston, MA
[5]Department of Surgery and Schulze Diabetes Institute, University of Minnesota School of Medicine, Minneapolis, MN
[6]Division of Pediatric Endocrinology, Department of Pediatrics, University of Minnesota Medical School, Minneapolis, MN
[7]Departments of Internal Medicine (Endocrinology) and Cellular & Molecular Physiology, Yale University, New Haven, CT
[8]Molecular Biology Institute, University of California, Los Angeles, Los Angeles, CA

Corresponding author: Marc Liesa, mliesa@mednet.ucla.edu, and Orian S. Shirihai, oshirihai@mednet.ucla.edu

Received 16 April 2019 and accepted 11 November 2019

This article contains Supplementary Data online at http://diabetes.diabetesjournals.org/lookup/suppl/doi:10.2337/db19-0379/-/DC1.

E.P.T. and N.A. contributed equally to this work.

(NEFAs) by β-cell mitochondria (11,12). These findings support the notion that alterations in β-cell function and insulin content induced by excess NEFAs can drive fasting hyperinsulinemia independently of the presence of fasting hyperglycemia. However, the exact molecular mechanisms by which excess fat can stimulate insulin secretion at nonstimulatory concentrations of glucose (non–glucose-stimulated insulin secretion [NGSIS]) are largely unknown.

Mitochondria are essential for pancreatic β-cell function, integrating fuel utilization with the generation of multiple intracellular signals stimulating insulin release (13). At low glucose levels, mitochondria in pancreatic β-cells preferentially oxidize NEFAs to sustain energy supply and maintain a relatively low release of insulin (11,14). The subsequent rise in blood glucose after a meal catalyzes a shift in fuel preference in β-cell mitochondria to glucose-derived pyruvate as a primary oxidative substrate. Glucose metabolism drives insulin secretion through multiple mechanisms, including generation of the signaling molecules ATP, NADPH, malonyl-CoA, long-chain acyl-CoAs, glutamate, and mitochondrial guanosine triphosphate (GTP) (15–17). In addition to marked fuel flexibility, β-cell mitochondria also exhibit a relatively high level of proton leak compared with other cell types (18,19). Mitochondrial proton leak is defined as the fraction of oxygen consumption that does not contribute to ATP synthesis in coupled mitochondria (20). We have proposed that NEFA-induced mitochondrial proton leak in β-cells may license the generation of signals stimulating insulin secretion regardless of β-cell ATP demand (21), but the mechanism of how NEFAs trigger mitochondrial proton leak in the β-cell is not known.

NEFAs are potent activators of the mitochondrial permeability transition pore (mPTP), an inner mitochondrial membrane channel formed by dimers of ATP synthase that, among other functions, facilitate reentry of protons into the mitochondrial matrix (22,23). Opening of the mPTP is regulated by an array of molecules and proteins, but the most well-documented protein regulator of the mPTP is cyclophilin D (CypD), a matrix peptidyl-prolyl *cis-trans* isomerase that activates the mPTP (22,24–26). Despite a well-defined role for the mPTP in cell death (24), emerging research has emphasized a more physiological role for CypD and the mPTP (27). A number of studies have characterized the metabolic phenotype of whole-body and tissue-specific CypD knockout (KO) mice. We (28) and others (29) have shown that whole-body deletion of CypD improves glucose tolerance on an HFD, and these mice do not develop fasting hyperinsulinemia on an HFD (29). An mPTP-related proton leak has been identified in islets and β-cells (30), but the precise role of the mPTP in β-cell proton leak and whether the mPTP influences insulin secretion in obesity and prediabetes have not been well studied.

In this study, we show that a primary increase in mitochondrial proton leak is sufficient to stimulate NGSIS in mouse and human islets. An excess NEFA environment in vivo and ex vivo increases islet proton leak and NGSIS by activating the mPTP. Furthermore, we demonstrate that mPTP-mediated proton leak stimulates NGSIS, but not glucose-stimulated insulin secretion (GSIS), and does not require mitochondrial ATP synthesis to secrete insulin. Taken together, we have uncovered a novel pathway that selectively drives pancreatic islet NGSIS, which may be therapeutically exploited to reduce fasting hyperinsulinemia and potentially prevent type 2 diabetes.

RESEARCH DESIGN AND METHODS

Materials

Collagenase P, D-glucose, L-leucine, L-glutamine, oleate, palmitate, poly-D-lysine, and diazoxide were purchased from Sigma-Aldrich (St. Louis, MO). Carbonyl cyanide-4-(trifluoromethoxy) phenylhydrazone (FCCP) was purchased from Sigma-Aldrich and Enzo Life Sciences (Farmingdale, NY). Antimycin A was purchased from Enzo Life Sciences. DMSO was purchased from VWR (Radnor, PA). Fatty acid–free BSA was purchased from EMD Millipore (Billerica, MA). FBS was obtained from Life Technologies (Carlsbad, CA). Oligomycin (Oligo) A and BAPTA-AM were obtained from Calbiochem (San Diego, CA). Sodium pyruvate and Matrigel Matrix GFR Phenol Red-free were purchased from Corning Life Sciences (Corning, NY). Seahorse XF96 Spheroid Microplates, Seahorse XF96 Cell Culture Plates, Seahorse XF96 FluxPaks, Seahorse XF Calibrant Solution, and Seahorse XF Base Medium Minimal DMEM were acquired from Agilent Technologies (Santa Clara, CA). BAM15 was a gift from Dr. Kyle Hoehn (University of New South Wales, Sydney, New South Wales, Australia). NIM811 was acquired from Janssen Pharmaceuticals (Horsham, PA).

Animals

C57BL/6J mice were obtained from The Jackson Laboratory. Nine-week-old male C57BL/6J mice were put on a custom diet from Research Diets (D09100310) containing 40% fat, 20% fructose, and 2% cholesterol or a control diet (PicoLab Rodent Diet 20 5053) for 4–15 weeks. Eighteen- to 20-week-old male C57BL/6N mice fed an HFD (60% HFD, D12492; Research Diets, New Brunswick, NJ) and control mice fed a chow diet (NIH-31M diet) were purchased from Taconic Biosciences. Whole-body CypD KO and littermate wild-type (WT) mice were produced from heterozygous breeding pairs derived from a male KO mouse (stock #009071, B6;129-Ppif^{tm1Jmol}/J; The Jackson Laboratory [25]) and a female WT control mouse (stock #101045, B6129SF2/J; The Jackson Laboratory). All animal care was in accordance with National Institutes of Health guidelines and University of California, Los Angeles (UCLA), institutional animal care and use committee approval (UCLA protocol #16–018). Mice were housed at the UCLA Animal Resources Facility in a 12-h/12-h light-dark cycle and maintained at 20–22.2°C. Animals were provided water and food ad libitum until the day of islet isolation.

Islet Isolation

Islets were isolated from 10–30-week-old mice through collagenase P injection into the bile duct, as previously

described (18,31), with minor modifications. Briefly, excised pancreata were digested in a 37°C water bath for 8–10 min, and the digested tissue was washed with RPMI medium containing 1% fatty acid–free BSA. Isolated islets were then cultured overnight at 37°C in 5% CO_2 in mouse islet medium (11 mmol/L glucose RPMI medium + 10% FBS + 100 units/mL penicillin, and 100 μg/mL streptomycin) before experiments.

Human Islets

Human islets were obtained from the University of Minnesota Schulze Diabetes Institute, as previously described (32). Briefly, islets were isolated from living donors with pancreatitis undergoing total pancreatectomy with islet autotransplantation (TPIAT) (see Table 1 for information regarding donors). Respirometry and insulin secretion were conducted at UCLA 1–2 days post-TPIAT.

Human samples were collected between October 2017 and October 2019 from participants in a prospective single-center institutional review board–approved protocol on TPIAT at the University of Minnesota. Informed consent was obtained from study participants for general study participation and for pancreatic tissue analyses.

Preparation of Fatty Acids

To make oleate/palmitate (OP) solutions, palmitic acid (P0500; Sigma) was first dissolved in DMSO to make a 51.7 mmol/L stock. Next, oleic acid (112–80–1; Sigma) was dissolved directly in the palmitate stock to make a 102 mmol/L oleate/51.7 mmol/L palmitate DMSO stock. This 2:1 OP stock or DMSO was then complexed to FBS at 57°C while vortexing to produce a 1 mmol/L oleate/0.5 mmol/L palmitate stock with a final DMSO concentration of 0.5–1.0%, as previously described (8).

Insulin Secretion

Intact mouse islets were seeded in V-bottom 96-well plates (Thermo Fisher Scientific) at either 6 islets/well or individual islets in 1 μL/well of Matrigel (8.4 mg/mL protein), and insulin secretion was measured while following a previously established protocol (33). Islets were incubated at 37°C for 3 min to solidify the Matrigel, and 100 μL/well of warm mouse islet medium (11 mmol/L glucose) was added. Islets were incubated at 37°C in 5% CO_2 for ~45–60 min. Islets were then washed two times with 3 mmol/L glucose Krebs buffer with 0.5% BSA (32) and preincubated in fresh 3 mmol/L glucose Krebs for 30 min at 37°C. This was followed by a 45-min incubation in either 3 mmol/L or 16.7 mmol/L glucose Krebs solution for NGSIS or GSIS, respectively. Nutrients and/or compounds were diluted in Krebs buffer as described in the figure legends. NIM811-sensitive NGSIS in islets was calculated by subtracting the NGSIS values in the presence of NIM811 from the average DMSO control value and dividing this value by the DMSO control NGSIS and multiplying by 100.

Insulin Measurements

An HTRF insulin assay kit (Cisbio, Bedford, MA) consisting of a fluorescence resonance energy transfer–based sandwich immunoassay with Europium cryptate and allophycocyanin (XL665) antibodies was used to quantify insulin levels in the media from insulin secretion experiments (32). Insulin concentration of the samples was calculated from an insulin standard curve (0–20 ng/mL or 0–100 ng/mL).

Islet Respirometry

Seahorse XF24 or XF96 extracellular flux analyzers (Seahorse Bioscience, Billerica, MA) were used for intact mouse islet respirometry while following previously described methods (18,32,34) with minor modifications. For XF96 assays, mouse (1–25 per well) or human (1 per well) islets were seeded in 1 μL/well Matrigel in a poly-D-lysine–coated XF96 plate and size matched between conditions. Islets were incubated at 37°C for 3.5 min to solidify the Matrigel before the addition of 100–150 μL/well Seahorse assay media (XF Base Media Minimal DMEM, pH 7.4, supplemented with 3 mmol/L glucose and 0.1% FBS). Islets were incubated at 37°C for ~1 h before starting the assay. For port injections, indicated nutrients/compounds were injected in port A (final concentrations in figure legends) followed by Oligo (final concentration 4.5 μmol/L) in port B, FCCP diluted in a mixture of 80% sodium pyruvate and 20% of 1:1 L-leucine/L-glutamine (final concentration 1 μmol/L FCCP in 11.4 mmol/L sodium pyruvate and 2.9 mmol/L each of leucine/glutamine) in port C, and antimycin A (final concentration 2.5 μmol/L) in port D. NIM811-sensitive proton leak in islets was calculated by subtracting the leak in the presence of NIM811 from the average DMSO control value and dividing this value by the DMSO control leak and multiplying by 100. Islets were imaged after Seahorse experiments using an Operetta high-throughput imaging device (PerkinElmer) in brightfield mode with 2× or 10× objectives.

Human Islet *Ppif* mRNA Expression

Human islet *Ppif* mRNA expression data expressed as $\log_2$ robust multiarray average values and donor BMI values were obtained from the National Center for Biotechnology Information Gene Expression Omnibus database (original sources from Taneera and colleagues [35–37]).

Statistics

Data are expressed as means ± SEM of at least three independent experiments or animals per group or three technical replicates per condition. *P* values were calculated by unpaired two-tailed *t* test, one-way ANOVA with Sidak or Dunnett multiple comparisons test, two-way

Table 1—Clinical parameters of University of Minnesota subjects undergoing TPIAT from which human islets were obtained and analyzed

Subject	Etiology	Pancreatitis duration (years)	Age (years)	Sex	BMI (kg/m^2)	Diabetes	Fasting C-peptide (ng/mL)	Fasting glucose (mg/dL)	HbA_{1c} (%)
1	Idiopathic	1	62	F	29.55	Y	3.4	157	6.9
2	Idiopathic	3	50	F	28.30	N	1.5	88	5.6
3	Alcoholism	1	51	M	31.00	Y	5.8	156	7.6
4	Familial/hereditary	26	57	M	24.49	N	1.6	88	5.8
5	Familial/hereditary	4.5	7	M	18.33	N	0.9	82	5.4
6	Pancreas divisum	20	36	M	27.68	Y	4.8	118	5.8
7	Idiopathic	4	47	F	19.11	N	1.2	76	4.8
8	Idiopathic	3	42	F	27.30	N	1.2	94	4.6
9	Familial/hereditary	6	38	M	24.65	N	1.3	100	5.2
10	Idiopathic	14	34	F	23.32	N	0.9	89	4.5
11	Familial/hereditary	7	9	F	20.30	N	1.9	83	6.1
12	Pancreas divisum	4	23	M	22.10	N	1.1	84	5.2
13	Pancreas divisum	7	41	M	22.70	N	1.1	110	5.7
14	Familial/hereditary	1	15	F	24.50	N	2.1	73	5.2
15	Idiopathic	11	42	F	31.30	N	1.7	98	4.7
16	Familial/hereditary	4	21	F	25.10	N	7.1	100	5.4
17	Familial/hereditary	13	30	M	23.10	N	2.2	97	5.4

BMI, fasting C-peptide, fasting glucose, and HbA_{1c} were measured ≤3 months before TPIAT procedure.

ANOVA with Tukey multiple comparisons test, or linear regression. Statistical significance was set at $P < 0.05$.

Data and Resource Availability

The data sets generated and/or analyzed during the current study are available from the corresponding author upon reasonable request. Components of the Seahorse XF96 individual islet analysis platform used during the current study are commercially available. No novel applicable resources were generated or analyzed during the current study.

RESULTS

Mitochondrial Proton Leak Drives NGSIS

Mitochondrial proton leak can be quantified by determining the fraction of islet mitochondrial respiration that is insensitive to mitochondrial ATP synthesis inhibition by Oligo (38) and can be normalized to basal respiration (Fig. 1*A*). Previous work has suggested that the inherently high proton leak in pancreatic β-cell mitochondria may amplify GSIS (18,19,21). However, it is not known whether mitochondrial proton leak per se is sufficient to increase insulin secretion at nonstimulatory concentrations of glucose (NGSIS) at 3 mmol/L glucose. To address this, we induced proton leak in isolated mouse islets incubated in 3 mmol/L glucose with the small molecule protonophore BAM15 (Fig. 1*A*), which selectively shuttles protons across the inner mitochondrial membrane without affecting the plasma membrane proton gradient (39). We found that 1 μmol/L stimulates proton leak without completely removing the control over respiration executed by the mitochondrial ATP synthase, as shown by the response of BAM15-treated islets to *1*) the ATP synthase inhibitor Oligo (Fig. 1*A*) and *2*) an additional uncoupler FCCP (Supplementary Fig. 1). Treatment with 1 μmol/L BAM15 doubled mitochondrial proton leak compared with DMSO vehicle (Fig. 1*B*). BAM15 increased islet NGSIS in a dose-dependent manner, with 1 μmol/L BAM15 inducing an approximately twofold increase in NGSIS (Fig. 1*C*).

Proton Leak–Mediated NGSIS Does Not Require Mitochondrial ATP Synthesis

To understand the relative mechanistic importance of mitochondrial proton leak in insulin release, we also investigated the interplay between proton leak and GSIS. Stimulatory glucose (16.7 mmol/L) increased mitochondrial proton leak (Supplementary Fig. 1) and elevated insulin secretion almost 30-fold over NGSIS (Fig. 1*D*). While BAM15-stimulated proton leak increased NGSIS, it caused the opposite effect on GSIS (Fig. 1*E*). Confirming this conclusion, blockade of mitochondrial ATP synthesis with Oligo decreased GSIS but had no effect on NGSIS (Fig. 1*E*). The only regulatory node of secretion at which NGSIS and GSIS converged was the K_{ATP} channel because its inhibition with diazoxide blocked both GSIS and NGSIS (Fig. 1*F*).

Inhibition of CypD Reduces NEFA-Mediated Proton Leak and NGSIS in Mouse Islets

Higher NGSIS observed in prediabetes is believed to be mediated by an increase in intracellular NEFA actions in the β-cell (12,40) as well as by signaling transduced by the plasma membrane free fatty acid receptor GPR40 (41,42). In this context, the links among increased NEFA, NGSIS, and mitochondrial proton leak are unclear. Therefore, we sought to determine whether conditions mimicking hyperlipidemia and insulin resistance in mice could increase mitochondrial proton leak and NGSIS in isolated mouse islets. Acute treatment of mouse islets with a 2:1 mixture of OP significantly increased proton leak (Fig. 2*A*–*C*) and NGSIS (Fig. 2*B* and *C*). We next aimed to identify the molecular entity responsible for NEFA-induced islet proton leak and NGSIS. NEFAs can trigger the opening of the mPTP (43), an inner mitochondrial membrane channel that facilitates reentry of protons into the mitochondrial matrix (22). The overall structure and components of the mPTP are still under active investigation, but the most well-documented regulator of the mPTP is the mitochondrial matrix isomerase CypD (25,26,44). Binding of CypD to the mPTP promotes pore opening, while inhibition of CypD markedly delays mPTP opening (25).

To determine whether the mPTP was responsible for islet proton leak, we treated islets with the nonimmunosuppressive cyclosporine-derived CypD inhibitor NIM811 (45). Pharmacological inhibition of CypD with NIM811 significantly reduced both proton leak (Fig. 2*D* and *E*) and NGSIS (Fig. 2*F* and *G*) induced by NEFAs without altering basal or maximal respiration (Supplementary Fig. 2). Importantly, in the absence of NEFAs, NIM811 did not affect NGSIS (Fig. 2*H*). Furthermore, NIM811 did not alter GSIS from mouse islets (Fig. 2*I*).

To confirm the involvement of CypD in proton leak–mediated insulin secretion, we isolated islets from mice lacking CypD (CypD KO) (25) or with 50% reduction in CypD (CypD Het). Deletion of CypD is a validated model for inhibition of PTP opening by increasing the threshold for activators to open the pore (46). Islets from CypD KO and CypD Het mice showed similar proton leak (Fig. 3*A*)

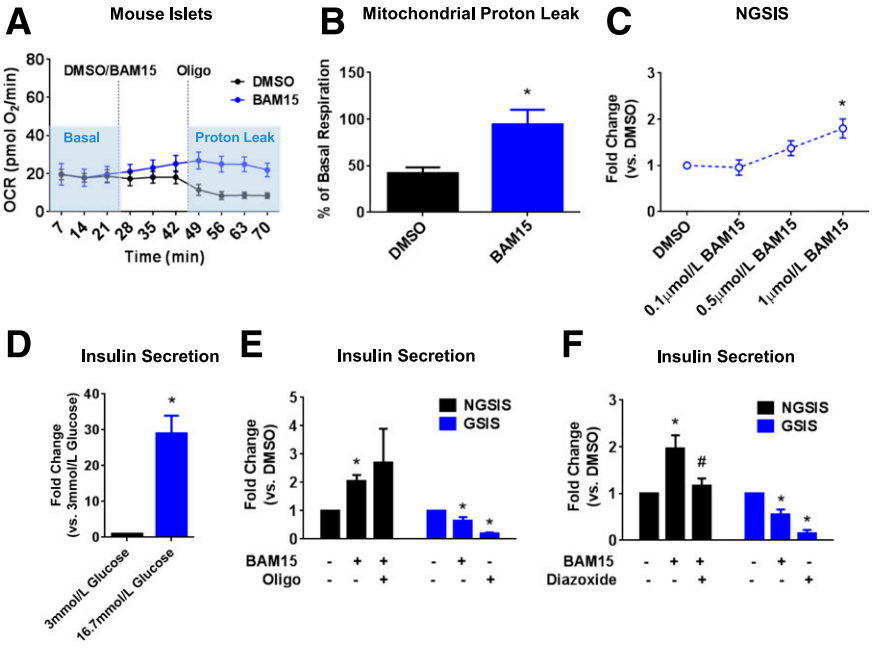

Figure 1—Proton leak drives NGSIS independently of mitochondrial ATP synthesis. *A*: Representative oxygen consumption rate (OCR) traces showing pharmacological stimulation of proton leak in isolated mouse islets. Islets were acutely exposed to 3 mmol/L glucose Seahorse media in the absence (DMSO) or presence of the mitochondrial protonophore BAM15 (1 μmol/L). Oxygen consumption under Oligo (proton leak) is normalized to the basal respiration after subtraction of nonmitochondrial respiration (n = 3 wells per condition from one experiment). *B*: Quantification of proton leak from mouse islets exposed to DMSO or 1 μmol/L BAM15. Proton leak is normalized to basal respiration (n = 3 independent experiments). *C*: Dose-dependent stimulation of NGSIS by BAM15. Mouse islets were treated with DMSO or BAM15 (0.1–1 μmol/L) diluted in 3 mmol/L glucose Krebs, and insulin secretion was quantified after 45 min (n = 3–10 independent experiments). *D*: Insulin secretion at 3 mmol/L glucose (NGSIS) or 16.7 mmol/L glucose (GSIS) in isolated mouse islets. GSIS is expressed as fold increase normalized to NGSIS (n = 12 independent experiments). *E*: NGSIS or GSIS from mouse islets in the absence or presence of 1 μmol/L BAM15 or 4.5 μmol/L Oligo (n = 3–8 independent experiments). *F*: NGSIS or GSIS in the absence or presence of 1 μmol/L BAM15 or 250 μmol/L diazoxide (n = 3–4 experiments). Data are mean ± SEM. *$P < 0.05$ by unpaired two-tailed t test (*B* and *D*), $P < 0.05$ compared with DMSO vehicle by one-way ANOVA (*C* and *E*), or significant difference compared with corresponding DMSO (*F*); #significant difference compared with corresponding BAM15 by one-way ANOVA.

and NGSIS (Fig. 3*B*) compared with WT islets in the absence of NEFAs. NEFAs were unable to induce proton leak in CypD KO islets to the same degree as in WT islets (Fig. 3*C*). CypD Het islets had a mild but not significant reduction in NEFA-stimulated proton leak (Fig. 3*C*). Islets from both CypD KO and CypD Het mice had significantly diminished NGSIS with NEFAs compared with WT controls (Fig. 3*D*). NIM811 only decreased NGSIS in WT but not in CypD KO or CypD Het islets (Fig. 3*D*), consistent with NIM811 targeting CypD. CypD deletion did not alter maximal or glucose-stimulated respiration (Supplementary Fig. 3), glucose-stimulated proton leak (Fig. 3*E*), or GSIS (Fig. 3*F*).

CypD-Dependent Proton Leak Drives NGSIS in Islets From Diet-Induced Obese Mice

CypD mRNA is increased in islets from subjects with prediabetes and diabetes who exhibit elevated NGSIS (35,36). Therefore, it is possible that CypD in the islet may contribute to the aberrantly high NGSIS observed in diet-induced obesity. To determine whether CypD contributed to basal hypersecretion of insulin in obesity, we first measured mitochondrial proton leak in islets isolated from lean WT mice and WT mice fed an HFD with higher NGSIS (Supplementary Fig. 4). Islets from diet-induced obese mice had significantly higher mitochondrial proton leak than islets from lean controls (Fig. 4*A*). Remarkably, proton leak showed a strong correlation with NGSIS in islets from HFD-fed but not from chow-fed lean mice (Fig. 4*B*). Given the role of CypD in NEFA-induced NGSIS, we rationalized that the higher proton leak and NGSIS in obesity may be prevented through pharmacological targeting of CypD with NIM811. Islets from obese mice showed significantly higher NIM811-sensitive proton leak (Fig. 4*C*) and NGSIS (Fig. 4*D*) than lean mice.

We used a Western diet as an additional model of diet-induced hyperglycemia and insulin resistance associated with higher NGSIS to further investigate whether proton leak drives NGSIS in islets from obese mice (Supplementary Fig. 4). Similar to the HFD model, islets isolated from mice fed a Western diet showed significantly higher mitochondrial proton leak than mice fed a control chow diet (Fig. 4*E*), and this leak positively correlated with islet NGSIS only in islets from obese mice (Fig. 4*F*). Islets from mice fed a Western diet showed significantly higher NIM811-sensitive proton leak (Fig. 4*G*) and NGSIS (Fig. 4*H*) compared with islets from chow-fed mice.

Mitochondrial matrix calcium is a potent signal activating mPTP opening (22,23). Depletion of intracellular calcium with BAPTA-AM inhibited NEFA-stimulated proton leak in islets of WT mice but had no effect in islets from CypD KO mice (Fig. 4*I*). BAPTA-AM had no effects in islets of chow-fed control mice (Fig. 4*J* and *K*) but decreased both proton leak and NGSIS of islets from obese mice fed a Western diet (Fig. 4*L* and *M*).

Proton Leak–Mediated NGSIS Activated by NEFAs Is Conserved in Human Islets

To test whether proton leak mediates NGSIS in isolated human islets, we obtained islets derived from living human donors undergoing TPIAT (32). Donor islets had an average glucose stimulation of about fivefold over basal (Fig. 5*A*). Similar to mouse islets, BAM15 significantly increased NGSIS in human islets incubated at 3 mmol/L glucose (Fig. 5*B*). NEFAs stimulated proton leak and NGSIS in human islets (Fig. 5*C*) to a similar extent as observed in mouse islets. NIM811 blocked NEFA-stimulated NGSIS in human islets (Fig. 5*D*).

We then measured the contribution of CypD to NEFA-mediated proton leak in human islets incubated in 6.7 mmol/L glucose, matching the elevated fasting blood glucose measured in an islet donor with prediabetes. NEFAs increased both proton leak (Fig. 5*E*) and NGSIS (Fig. 5*F*) in a manner partially dependent on CypD at 3 mmol/L and 6.7 mmol/L glucose. As expected, fasting C-peptide, a surrogate marker for insulin secretion in vivo, tended to be higher in TPIAT patients with higher BMI (Fig. 5*G*). Fasting C-peptide was also positively correlated with fasting LDL cholesterol (LDL-C) (Fig. 5*H*), consistent with high LDL-C being a common hallmark of the metabolic syndrome. Fasting C-peptide (Fig. 5*I*), BMI (Fig. 5*J*), and fasting LDL-C (Fig. 5*K*) were positively correlated with NEFA-activated proton leak in islets from a small cohort of TPIAT patients. On the other hand, NEFA-activated proton leak showed no correlation with fasting blood glucose (Fig. 5*L*) or HbA_{1c} (Fig. 5*M*). Since elevated fasting C-peptide, high BMI, and increased circulating LDL-C are markers predicting a high risk of developing type 2 diabetes, we mined previously published human islet transcriptomics data (35–37) to investigate whether susceptibility of PTP opening driven by CypD changed in the progression of type 2 diabetes. *Ppif* expression was significantly higher in islets from donors with type 2 diabetes than from donors without diabetes (Fig. 5*N*). *Ppif* expression tended to be higher in obese (BMI >27 kg/m^2) donors with diabetes than in obese donors without diabetes (Fig. 5*O* and *P*).

Individual Islet Analysis Reveals Heterogeneity in Proton Leak and NGSIS in Human Islets

Pancreatic islets and β-cells within islets show immense heterogeneity in mitochondrial function (32,47,48), a phenomenon that is an important factor in the progression of diabetes (49). Upon closer examination of mouse islets, proton leak varied considerably among islet wells, especially in obesity (Fig. 6*A*). Similarly, islets from obese mice showed a greater range in insulin secretion up to 2 ng/mL per islet (Fig. 6*B*), and roughly 66% of obese islets had greater leak or NGSIS than the average chow-fed control islets (Fig. 6*C*).

Therefore, we hypothesized that a small portion of islets within a population may be responsible for the increased proton leak and enhanced NGSIS observed in obesity. We have previously developed in collaboration with Agilent

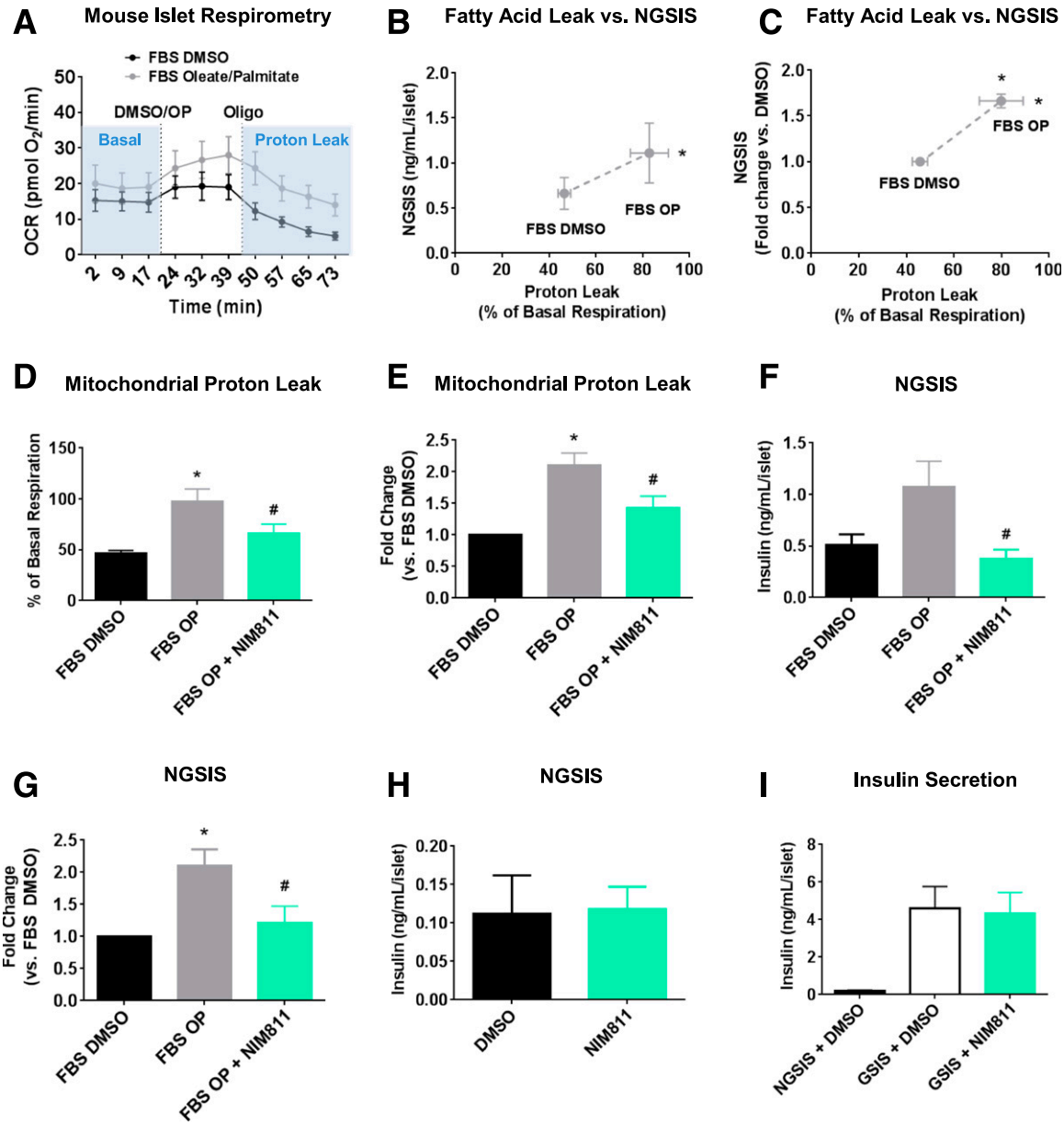

Figure 2— Pharmacological inhibition of CypD reduces NEFA-stimulated proton leak and NGSIS in mouse islets. *A*: Representative Seahorse XF96 oxygen consumption rate (OCR) traces showing proton leak measurements in isolated mouse islets treated with NEFAs. Islets were acutely exposed to OP (150 μmol/L oleate/75 μmol/L palmitate) complexed to FBS or FBS complexed to DMSO diluted in 3 mmol/L glucose, and proton leak was determined as measured in Fig. 1 ($n = 4$ wells for DMSO and 3 wells for OP derived from one experiment). *B* and *C*: Comparison of OP-stimulated proton leak and NGSIS in mouse islets. NEFA-stimulated proton leak is normalized to basal OCR, and NEFA-stimulated NGSIS was expressed as ng/mL/islet (*B*) or normalized to FBS DMSO (*C*) ($n = 6$ [proton leak] or 5 [NGSIS] independent experiments). *D* and *E*: Mitochondrial proton leak in mouse islets acutely exposed to OP in the absence (DMSO) or presence of the CypD inhibitor NIM811 (1 μmol/L). Islets were pretreated with DMSO or NIM811 in Seahorse media containing 3 mmol/L glucose for 1 h before respirometry. Proton leak is normalized to basal respiration (*D*) or expressed as fold change vs. DMSO control (*E*) ($n = 6$–8 independent experiments). *F* and *G*: OP-mediated NGSIS from NIM811-treated islets. Mouse islets were pretreated for 30 min in 3 mmol/L Krebs containing DMSO or 1 μmol/L NIM811. Islets were then switched to 3 mmol/L glucose Krebs with DMSO, OP, or OP + NIM811, and insulin secretion was measured after 45 min. Data are expressed as ng/mL/islet (*F*) or normalized to FBS DMSO (*G*) ($n = 6$–11 independent experiments). *H*: NGSIS in the absence of OP from islets treated with vehicle (DMSO) or NIM811 ($n = 3$ independent experiments). *I*: GSIS in the absence or presence of NIM811. Islets were pretreated with DMSO or 1 μmol/L NIM811 in 3 mmol/L glucose Krebs for 30 min. Islets were then exposed to 16.7 mmol/L glucose Krebs buffer in the absence (DMSO) or presence of NIM811 for 45 min ($n = 3$ independent experiments). Data are mean ± SEM. *$P <$ 0.05 by two-tailed unpaired *t* test (*B* and *C*) or significant difference compared with DMSO (*D*, *E*, and *G*); #significant difference compared with OP by one-way ANOVA.

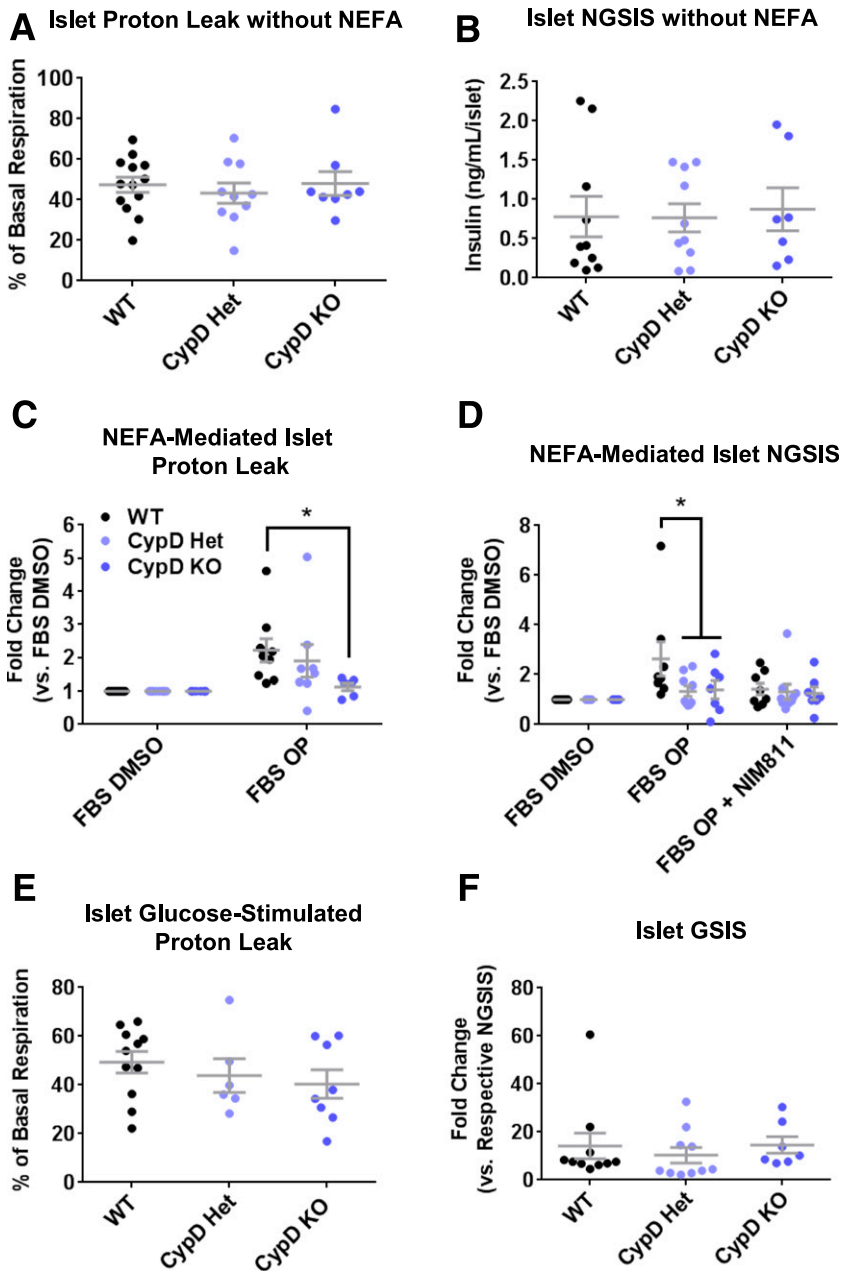

Figure 3—Genetic reduction of CypD expression decreases NEFA-induced proton leak and NGSIS in mouse islets. *A*: Basal mitochondrial proton leak in islets from CypD KO, CypD Het, or WT littermate mice in the absence of OP. Proton leak is normalized to basal respiration (n = 13 WT, 10 Het, and 8 KO mice). *B*: NGSIS in the absence of OP from islets of CypD KO, CypD Het, or WT mice (n = 7, 10, and 10 mice, respectively). *C*: OP-stimulated proton leak in CypD KO, CypD Het, and WT mice. Mouse islets were acutely exposed to OP or FBS DMSO control in 3 mmol/L glucose, and proton leak was measured as noted in Fig. 2 (n = 9 WT, 8 Het, and 6 KO mice). *D*: OP-mediated NGSIS in islets from CypD KO, CypD Het, or WT mice. Individual mouse islets were pretreated for 30 min in 3 mmol/L Krebs containing DMSO or 0.1 μmol/L NIM811. Islets were then switched to 3 mmol/L glucose Krebs with DMSO, OP, or OP + NIM811, and insulin secretion was measured after 45 min. Data are normalized to DMSO (n = 8 WT, 9 Het, and 7 KO mice). *E*: Glucose-stimulated proton leak from islets of CypD KO, CypD Het, or WT mice. Islets were acutely exposed to 20 mmol/L glucose, and proton leak was calculated as noted in Figs. 1 and 2 (n = 11 WT, 6 Het, and 8 KO mice). *F*: GSIS from CypD KO, CypD Het, and WT islets. Data are normalized to each genotype's respective basal insulin secretion at 3 mmol/L glucose (n = 10 WT, 10 Het, and 7 KO mice). Data are mean ± SEM. *$P < 0.05$ compared with WT FBS OP by two-way ANOVA.

Technologies a new islet respirometry method (32) enabling the bioenergetic profiling of large-sized individual mouse and human islets. Here, we have augmented this novel technique by embedding individual human islets in Matrigel in wells of a regular XF96 Seahorse cell culture plate (Fig. 6*D* and *E*), enabling the profiling of mitochondrial bioenergetics in smaller individual islets from populations of human islets (Supplementary Fig. 5). Our analyses revealed remarkable

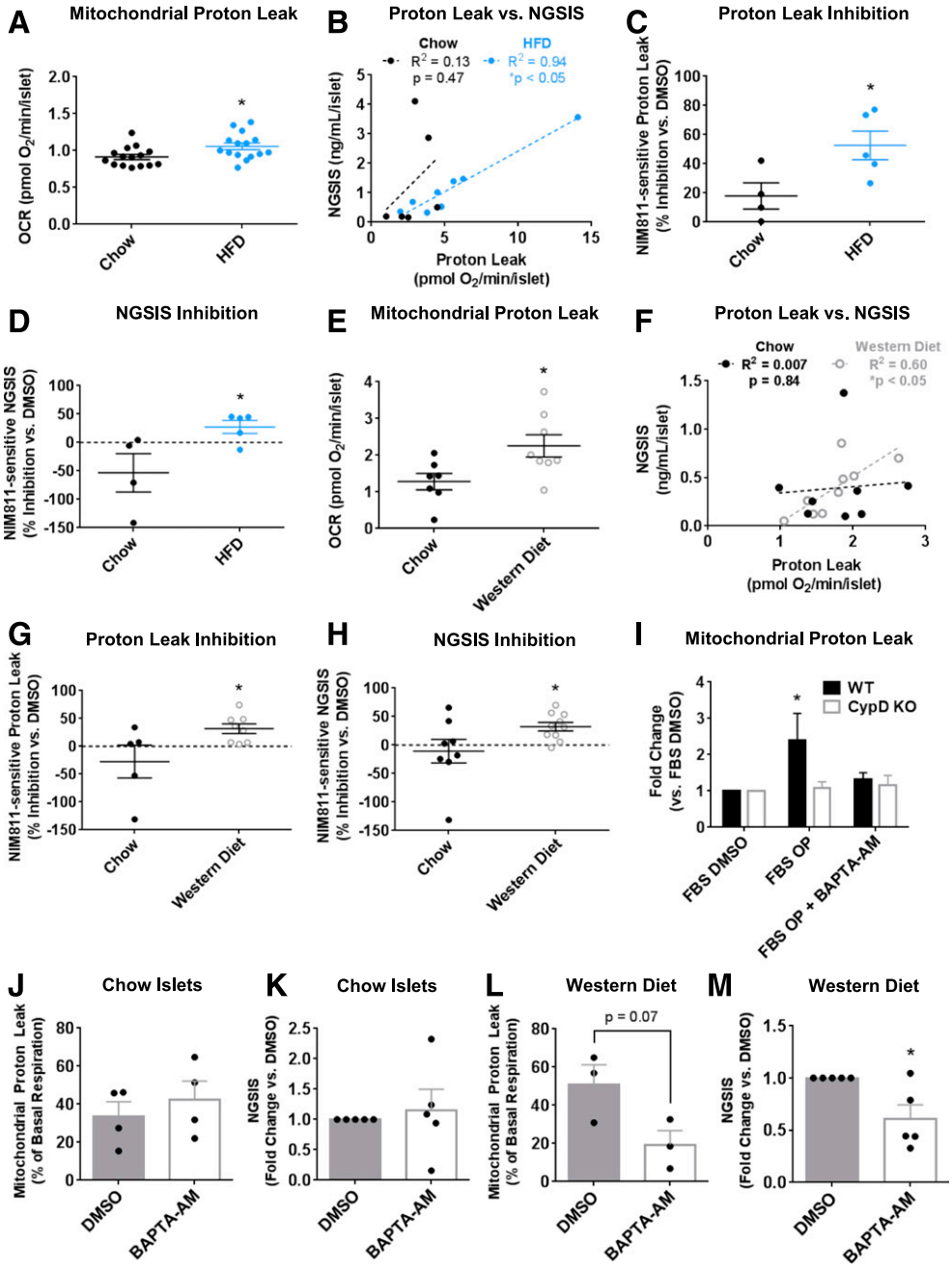

Figure 4—CypD-dependent proton leak drives NGSIS in islets from diet-induced obese mice. *A*: Mitochondrial proton leak in islets isolated from mice fed a chow diet or an HFD for 12 weeks. Proton leak is normalized per islet ($n = 15$ mice per diet). *B*: Correlation between proton leak (pmol O_2/min/islet) and NGSIS (ng/mL/islet) at 3 mmol/L glucose in isolated chow- or HFD-fed mouse islets ($n = 6$ and 8 mice, respectively). R^2 values determined through linear regression. *C*: NIM811-sensitive proton leak in islets from chow- or HFD-fed mice for 12–28 weeks. NIM811 sensitivity was calculated as noted in the RESEARCH DESIGN AND METHODS section ($n = 4$ chow or 5 HFD independent experiments). *D*: NIM811-sensitive NGSIS of islets isolated from chow- or HFD-fed mice ($n = 4$ and 5 mice, respectively). *E*: Mitochondrial proton leak from islets of mice fed a Western diet (high fat/cholesterol diet) or chow control diet for 7–14 weeks ($n = 8$ and 7 mice, respectively). *F*: Comparison of proton leak and NGSIS in islets isolated from mice fed a Western or chow control diet for 7–14 weeks ($n = 9$ and 8, respectively). R^2 values determined through linear regression. *G*: NIM811-sensitive proton leak of islets from chow- or Western diet-fed mice ($n = 5$ and 7 mice, respectively). *H*: NIM811-sensitive NGSIS of chow or Western diet mouse islets ($n = 8$ and 10 mice, respectively). Islets were treated with 0.1 μmol/L NIM811 in *G* and *H*. *I*: Mitochondrial proton leak of chow-fed CypD KO or littermate WT control mouse islets in the absence or presence of OP or 100 μmol/L BAPTA-AM. Islets were pretreated with DMSO or BAPTA-AM in 3 mmol/L glucose for 1 h at 37°C before respirometry ($n = 4$ WT and 3 KO experiments). *J* and *K*: Proton leak and NGSIS of mouse islets isolated from mice fed chow diet for 14–15 weeks in the absence or presence of BAPTA-AM ($n = 4$ mice for leak and 5 mice for NGSIS). *L* and *M*: Proton leak and NGSIS of BAPTA-AM–treated islets isolated from mice fed a Western diet for 14–15 weeks ($n = 3$ mice for leak and 5 mice for NGSIS). Data are mean ± SEM. *$P < 0.05$ by unpaired two-tailed *t* test (*A*, *C–E*, *G*, *H*, and *M*), for a nonzero slope by linear regression (*B* and *F*), or compared with FBS DMSO by two-way ANOVA (*I*). OCR, oxygen consumption rate.

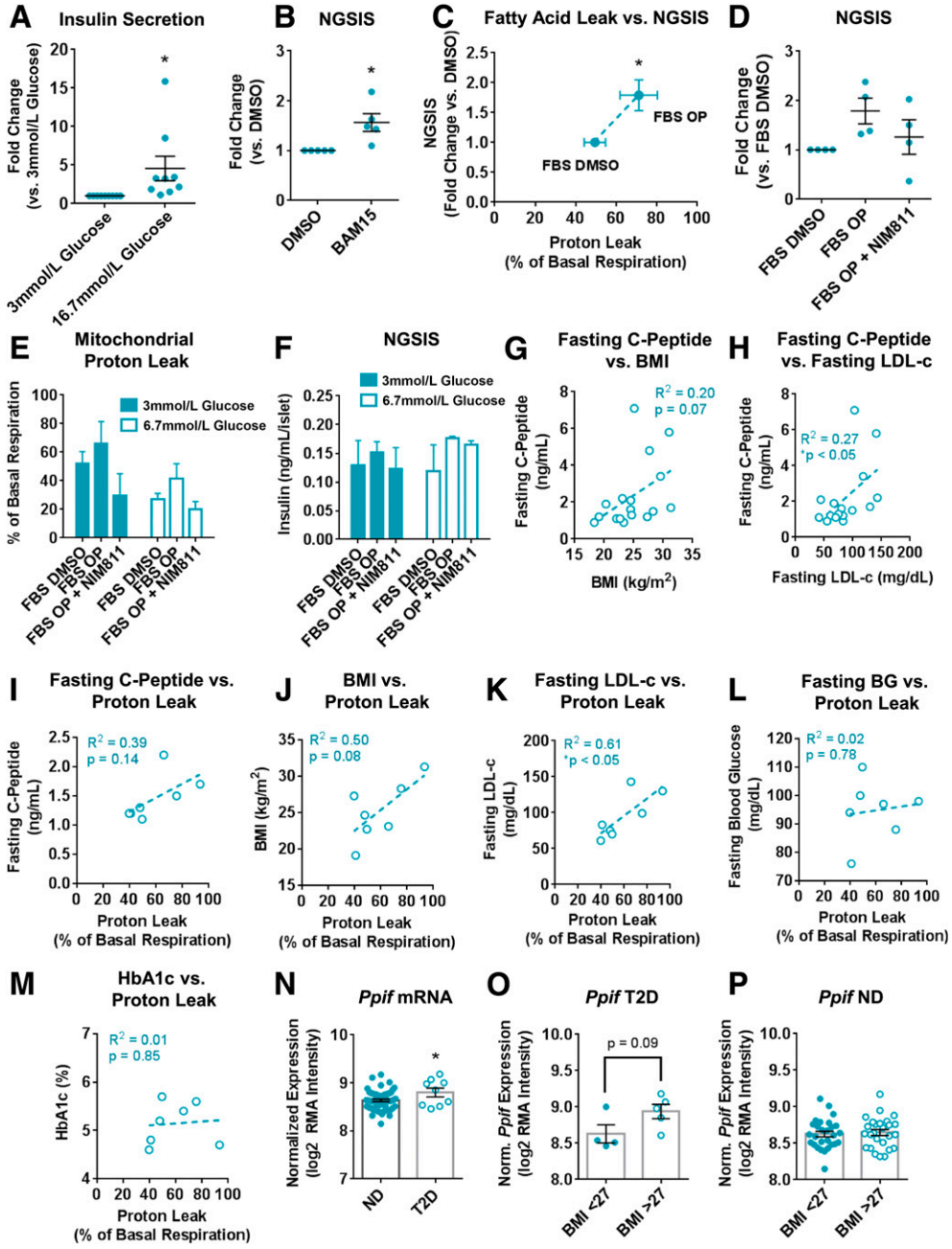

Figure 5—Proton leak–stimulated NGSIS is conserved in human islets. *A*: GSIS of human islets expressed as fold change compared with 3 mmol/L glucose ($n = 9$ donors). *B*: Proton leak–mediated NGSIS in individual human islets treated with 1 μmol/L BAM15 in 3 mmol/L glucose Krebs. Data are normalized to DMSO vehicle ($n = 5$ donors). *C*: Comparison of mitochondrial proton leak and NGSIS of human islets in the presence of OP. Proton leak is normalized to basal respiration, and NGSIS is normalized to FBS DMSO control ($n = 4$ donors). *D*: NEFA-mediated NGSIS in human islets in the absence or presence of 0.1 μmol/L NIM811. Data are normalized to FBS DMSO control ($n = 4$ donors). *E*: Mitochondrial proton leak of human islets in the absence or presence of OP or 0.1 μmol/L NIM811 at 3 or 6.7 mmol/L glucose, the fasting blood glucose of the human subject before TPIAT surgery ($n = 4$–6 wells per condition from one human donor). *F*: NGSIS from islets of the same donor as in *E* in the absence or presence of OP or 0.1 μmol/L NIM811 at 3 or 6.7 mmol/L glucose ($n = 3$ wells per condition). *G* and *H*: Relationship between fasting C-peptide and BMI or fasting LDL-C of human subjects before TPIAT surgery ($n = 16$–17 donors). R^2 value determined through linear regression. *I*–*M*: Relationship between average OP-stimulated proton leak of human islets measured ex vivo in 3 mmol/L glucose and fasting C-peptide, BMI, fasting LDL-C, fasting blood glucose (BG), or HbA_{1c} measured in human subjects before TPIAT surgery ($n = 7$ donors). R^2 value determined through linear regression. *N*: *Ppif* mRNA expression in islets from donors with no diabetes (ND) or with type 2 diabetes (T2D) ($n = 54$ and 9, respectively). *O* and *P*: Islet *Ppif* mRNA expression binned by BMI (cutoff 27 kg/m^2, range 17.6–36.9 kg/m^2) in donors with T2D or ND ($n = 28$ [BMI <27 kg/m^2] and 26 [BMI >27 kg/m^2] for ND and 4 donors [BMI <27 kg/m^2] and 5 [BMI >27 kg/m^2] donors for T2D). Data analyzed by unpaired two-tailed *t* test. Data are mean ± SEM. Human islets were obtained from living donors with pancreatitis after TPIAT at the University of Minnesota Schulze Diabetes Institute. *Ppif* mRNA data were reanalyzed from Taneera and colleagues (35–37). *$P < 0.05$ compared with two-tailed unpaired *t* test (*A*–*C* and *N*) or for a nonzero slope by linear regression (*H* and *K*). Norm., normalized; RMA, robust microarray analysis.

heterogeneity in proton leak among individual human islets in the absence (Fig. 6*F*) and presence (Fig. 6*G*) of NEFAs. Treatment of human islets with NEFAs increased overall proton leak, but not all islets responded to NEFAs (Fig. 6*H*).

We then measured NGSIS from individual human islets after incubation with 200 μmol/L oleate/100 μmol/L palmitate, close to concentrations observed in obese humans (50). Treatment of individual human islets with OP increased NGSIS compared with FBS DMSO control (Fig. 6*I*). Similar to proton leak measurements, OP treatment increased the proportion of human islets with relatively higher insulin secretion (Fig. 6*J*). However, most islets displayed a marginal response to NEFAs (Fig. 6*I* and *J*). Taken together, our findings suggest that elevated circulating NEFAs in obesity can activate the PTP in pancreatic islets, which drives increased insulin release at low glucose levels (Fig. 6*K*).

DISCUSSION

Fasting hyperinsulinemia occurs well before diagnosis of overt type 2 diabetes, yet no therapeutic interventions currently exist that specifically target this metabolic defect. Drugs that reduce insulin secretion by targeting the K_{ATP} channel in β-cells (51,52) or mimicking the insulin secretion-blocking hormone somatostatin (53) have shown promise in lowering body weight and improving glucose homeostasis. However, these drugs do not discriminate between NGSIS and GSIS. This scarcity of therapeutic options can mainly be attributed to a lack of knowledge regarding the mechanisms regulating insulin secretion that occur at nonstimulatory glucose levels (NGSIS). In this study, we have identified a molecular mechanism that contributes to NGSIS in both murine and human islets. We found that NGSIS in pancreatic islets is controlled by proton leak through the mPTP and does not require mitochondrial ATP synthesis to stimulate insulin secretion. Proton leak–dependent NGSIS is higher in islets from obese mice and can be inhibited through pharmacological targeting of the mPTP activator protein CypD with NIM811. To our knowledge, this is the first discovery of a druggable pathway that specifically regulates NGSIS and may provide a novel therapeutic approach to prevent fasting hyperinsulinemia.

Pancreatic β-cells and islets have an inherently high mitochondrial proton leak compared with other cell types (18), but the molecular entity responsible for this leak has been elusive for decades. Uncoupling protein 2 (UCP2) was proposed as the mediator of β-cell proton leak (54), but β-cell–specific deletion of UCP2 had no effect on islet proton leak (55). Exposure of islet β-cells to an obesogenic environment results in excessive NEFA availability and mitochondrial calcium overload (56), which is the perfect environment to activate the mPTP (22). Indeed, we observed that the proton leak gained in obesity or in the presence of mPTP-activating NEFAs is sensitive to inhibition by NIM811 and to genetic deletion of CypD. CypD and the mPTP have previously been studied in β-cells in vitro (57) and in vivo (58) but only in islet cell death. The mPTP is involved in more than just the demise of islet cells (30), as several physiological roles have been recently discovered (59).

Our work highlights a pathophysiological role for the mPTP in β-cells regulating NGSIS in obesity. Whole-body CypD KO mice show improved glucose tolerance (28,29), increased glucose uptake into skeletal muscle, and enhanced liver glycogen storage when fed an HFD (28). However, muscle- or liver-specific deletion of CypD failed to recapitulate the metabolic benefits observed in the whole-body KO model (60). Given that whole-body deletion of CypD alters insulin levels in vivo (29) and ex vivo, it is plausible that the improved insulin sensitivity in the CypD KO mice on HFD is due to a reduction in proton leak–mediated NGSIS. However, measurement of islet proton leak and fasting insulin levels will have to be measured in mice lacking CypD specifically in β-cells to verify this hypothesis.

Despite the importance of mitochondrial function for GSIS, it is interesting that proton leak seems to only regulate NGSIS. NEFAs are known to alter mitochondrial function and elevate NGSIS through GPR40 signaling (41,42), but GPR40 signaling contributes to both NGSIS and GSIS pathways. Stimulatory glucose alone increased proton leak in pancreatic islets, but pharmacological and genetic inhibition of CypD only reduced proton leak and NGSIS in the presence of OP, with no effects on glucose-stimulated proton leak or GSIS. Since multiple entities facilitate proton leakage across the inner mitochondrial membrane (38), including the ADP/ATP carrier (61) and nicotinamide nucleotide transhydrogenase (62), it is possible that the proton leak activated by high glucose levels may be mediated through a different molecular target in the β-cell than the leak generated by NEFAs at low glucose levels.

Exactly how proton leak elicits insulin release is still unknown. Unlike GSIS, NGSIS is unique in that mitochondrial ATP synthesis does not play a major role. In obesity, we speculate that the elevated circulating NEFAs at fasting glucose levels activate the mPTP (43), increasing proton leak in β-cell mitochondria and driving tricarboxylic acid cycle flux to maintain mitochondrial membrane potential. This selective engagement of the mPTP is plausible because opening of the mPTP relies on the available metabolic substrate (63). Increased tricarboxylic acid cycle flux may promote production of a mitochondrial signaling metabolite, such as GTP (17,64). It is still unclear exactly how mitochondrial GTP promotes insulin secretion, but this process may depend on GTP-dependent PEPCK conversion of oxaloacetate to phosphoenolpyruvate (65). Phosphoenolpyruvate can be exported from mitochondria and used by pyruvate kinase to generate pyruvate and ATP near the K_{ATP} channel on the plasma membrane (66).

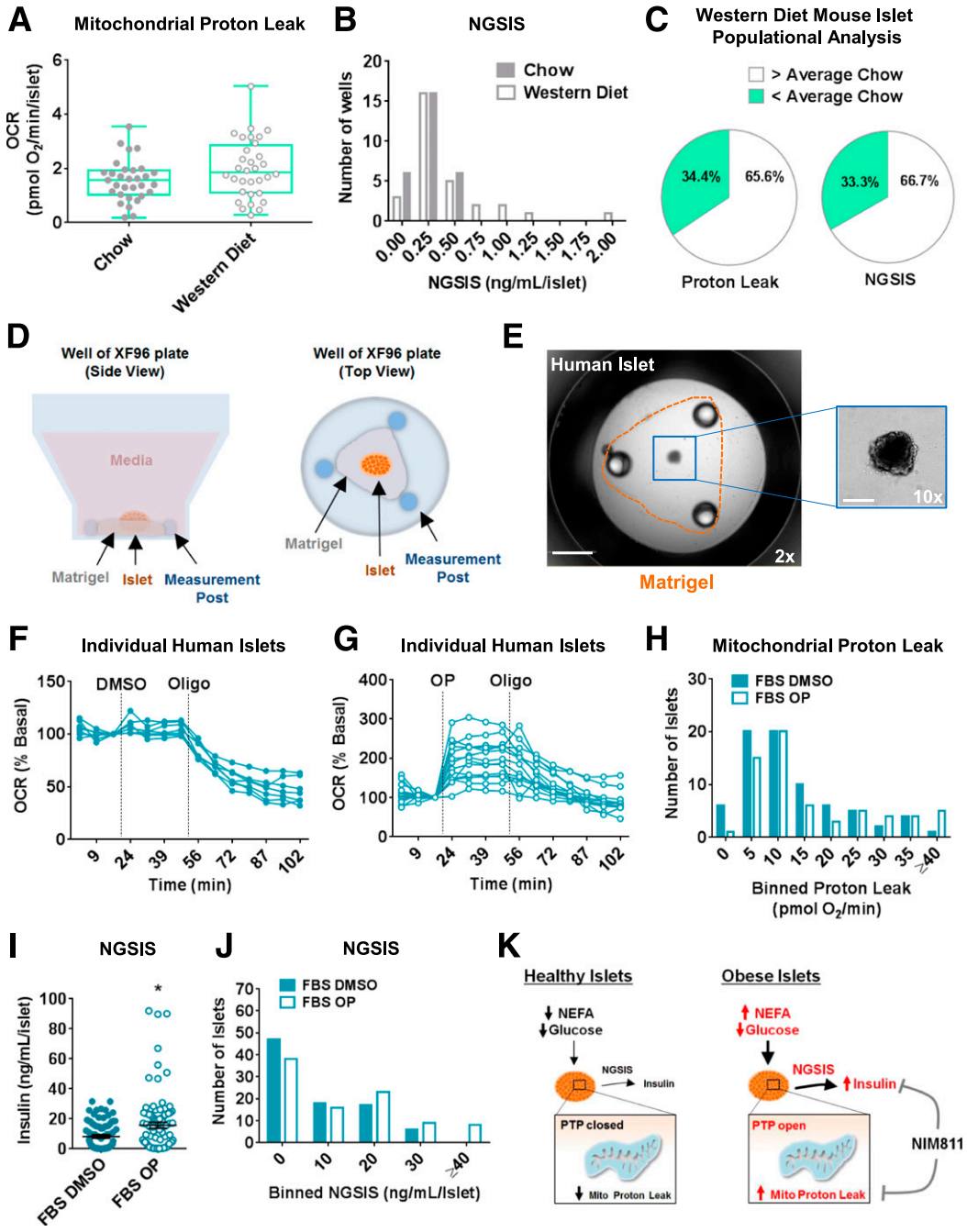

Figure 6—Individual islet analysis reveals heterogeneity in NEFA-stimulated proton leak and NGSIS in human islets. *A*: Box and whisker plots of mitochondrial proton leak of islets from chow- or Western diet–fed mice (7–14 weeks of diet). Each point represents a well with three islets ($n = 31$ wells from six experiments for chow and 32 wells from four experiments for Western diet). *B*: Binned NGSIS of chow or Western diet islets. Bin center = 0.25 ($n = 28$ wells for chow and 30 wells for Western diet). *C*: Pie charts showing the percentage of islets from obese mice with proton leak or NGSIS that is either less than or greater than the average lean chow islet values. Data are derived from *A* and *B*. *D*: Bioenergetics analysis of Matrigel-embedded individual human islets with the Seahorse XF96 cell culture plate. *E*: Brightfield image (original magnification ×2, scale bar = 1 mm) of an individual Matrigel-embedded human islet after a Seahorse assay. Matrigel is outlined in orange. Inset shows the same islet at original magnification ×10 (scale bar = 200 μm). *F* and *G*: Representative oxygen consumption rate (OCR) traces of individual Matrigel-embedded human islets measured in the Seahorse XF96 culture plate in the absence (*F*) or presence (*G*) of OP. Data are normalized to basal respiration ($n = 7$–14 islets from one human donor). *H*: Binned proton leak from individual human islets acutely exposed to either DMSO or OP. Proton leak is expressed as pmol O_2/min. Bin center = 5 ($n = 75$ islets for DMSO and 63 islets for OP from four human donors). *I*: NGSIS from individual human islets treated with 200 μmol/L oleate/100 μmol/L palmitate complexed to FBS or FBS DMSO control for 20 h. NGSIS is expressed as ng/mL/islet ($n = 88$ islets for DMSO and 94 islets from three human donors). *J*: Binned NGSIS of OP-treated islets from the same donors as in *I*. Bin center = 5 ($n = 88$ islets for DMSO and 94 islets from three human donors). *K*: In obesity, elevated NEFAs at low glucose levels activate PTP-dependent proton leak in pancreatic islets, which drives elevated NGSIS. Human islets were obtained from living donors with pancreatitis after TPIAT at the University of Minnesota Schulze Diabetes Institute. Data are mean (*C*) or mean ± SEM (*I*). *$P < 0.05$ by unpaired two-tailed *t* test. Mito, mitochondrial.

Currently, mPTP function is mainly studied using pharmacological and genetic tools that target the mPTP regulatory protein CypD. CypD is not a critical component of the pore but instead is a validated regulator that induces pore opening (22,25,26,46). The canonical mPTP inhibitor, cyclosporine A, simultaneously inhibits CypD and calcineurin, a phosphatase that controls inflammatory signaling and is also important for β-cell function (67). NIM811 efficiently blocks the ability of CypD to activate the pore without changing calcineurin (45) but inhibits all cyclophilins to some degree and can have other off-target effects (68). CypD ablation reduces the probability of mPTP activation by increasing the threshold for calcium-induced opening (22,25). Because both CypD deletion and NIM811 had similar inhibitory effects on NGSIS, the mPTP is most likely the major effector of NGSIS rather than other actions CypD might have on mitochondrial function.

Pancreatic islets exhibit remarkable functional heterogeneity in mitochondrial function (47) and insulin secretory capacity (32,69). By modifying our method for bioenergetic profiling of large-sized individual mouse and human islets (32), we have facilitated the measurement of mitochondrial proton leak of individual human islets within the population of multiple living donors. Individual bioenergetics analyses revealed marked heterogeneity in proton leak among individual human islets and highlighted a subpopulation of islets with higher sensitivity to NEFA-stimulated proton leak and NGSIS. Our observation of heterogeneous proton leak complements previous work showing that mPTP activity can vary widely between tissues (60). Since selective populations of islets are altered in the pancreas of individuals with type 2 diabetes (49), it is plausible that certain islets are more susceptible to NEFA-induced leak and NGSIS than others.

Fasting hypersecretion of insulin can drive obesity (9,70), insulin resistance (1), and the progression of diabetes (2–4). Mild reduction in insulin secretion can reverse obesity and improve glycemia (10,71); however, there are currently no small-molecule drugs that specifically target NGSIS without altering GSIS. In this study, we have identified a potential therapeutic target for lowering insulin levels at basal glucose levels in obesity and prediabetes. Of note, metformin, the most commonly prescribed drug for type 2 diabetes, also inhibits the PTP in β-cells (57) and restores NGSIS in rat islets exposed to excess fatty acids (72). With sufficient pharmacological validation and optimization, blockade of proton leak in the β-cell may provide a promising new avenue by which to halt progression of type 2 diabetes.

Acknowledgments. The authors thank Drs. Paolo Bernardi (University of Padova, Padova, Italy), Jude Deeney and Barbara Corkey (Boston University), Marc Prentki (Montreal Diabetes Research Center, Centre de Recherche du CHUM, Montreal, Quebec, Canada), Lisa Norquay (Janssen Pharmaceuticals, Spring House, PA), and Daniel Dagan (Technion Israel Institute of Technology, Haifa, Israel) for valuable feedback and discussion during the preparation of the manuscript. The authors also thank Dr. Kyle Hoehn (University of Virginia, Charlottesville, VA, and University of New South Wales, Sydney, New South Wales, Australia) for generously supplying BAM15 and Janssen Pharmaceuticals (Horsham, PA) for supplying NIM811. Finally, the authors are grateful to Dr. Yijun Chen (UCLA) for helping to coordinate and design the Western diet obesity mouse model.

Funding. N.A. was funded by a fellowship from Kuwait University. This project was supported by a grant from the Kuwait Foundation for the Advancement of Sciences under project code CB17-63 MM-01 awarded to N.A.; National Institutes of Health (NIH), National Institute for Diabetes and Digestive and Kidney Diseases (NIDDK), funding mechanism R01-DK-110181 awarded to R.G.K.; UCLA Department of Medicine Chair commitment and University of California, San Diego/UCLA Diabetes Research Center grant NIH P30-DK063491 awarded to M.L.; and NIH NIDDK funding mechanisms 5R01-DK-074778-10 and R01-DK-099618 and American Diabetes Association funding mechanism 1-19-IBS-049 awarded to O.S.S.

Duality of Interest. This project was supported by a Sponsored Research Agreement from Janssen Research and Development (UCLA code #2016-1342). E.P.T., M.L., and O.S.S. are cofounders of Enspire Bio, Inc., a drug discovery company currently developing inhibitors of proton leak–mediated insulin secretion for treatment of obesity and prediabetes. No other potential conflicts of interest relevant to this article were reported.

Author Contributions. E.P.T. and N.A. wrote the manuscript. E.P.T., N.A., S.B., J.D.W., E.R., S.S., K.E., J.L., and L.S. performed experiments and analyzed data. E.P.T., N.A., M.L., and O.S.S. edited the manuscript and revised the manuscript for resubmission. E.P.T. and S.B. performed experiments during the revision process. S.S., J.J.W., M.L., and O.S.S. contributed to the project conception. M.A., Z.S., and J.J.W. isolated and shipped islets from human patients with pancreatitis undergoing total pancreatectomy with islet autotransplantation at the University of Minnesota. M.D.B. obtained patient consent for human islet studies and evaluated patients before and after pancreas removal and islet transplantation. R.G.K. aided in experimental planning. M.L. and O.S.S. are the guarantors of this work and, as such, had full access to all the data in the study and take responsibility for the integrity of the data and the accuracy of the data analysis.

Prior Presentation. Parts of this study were presented in poster form at the 78th Scientific Sessions of the American Diabetes Association, Orlando, FL, 22–26 June 2018.

References

1. Gregory JM, Smith TJ, Slaughter JC, et al. Iatrogenic hyperinsulinemia, not hyperglycemia, drives insulin resistance in type 1 diabetes as revealed by comparison with GCK-MODY (MODY2). Diabetes 2019;68:1565–1576

2. Pories WJ, Dohm GL. Diabetes: have we got it all wrong? Hyperinsulinism as the culprit: surgery provides the evidence. Diabetes Care 2012;35:2438–2442

3. Erion K, Corkey BE. β-cell failure or β-cell abuse? Front Endocrinol (Lausanne) 2018;9:532

4. Nolan CJ, Prentki M. Insulin resistance and insulin hypersecretion in the metabolic syndrome and type 2 diabetes: time for a conceptual framework shift. Diab Vasc Dis Res 2019;16:118–127

5. Dankner R, Chetrit A, Shanik MH, Raz I, Roth J. Basal-state hyperinsulinemia in healthy normoglycemic adults is predictive of type 2 diabetes over a 24-year follow-up: a preliminary report. Diabetes Care 2009;32:1464–1466

6. Tricò D, Natali A, Arslanian S, Mari A, Ferrannini E. Identification, pathophysiology, and clinical implications of primary insulin hypersecretion in nondiabetic adults and adolescents. JCI Insight 2018;3:e124912

7. Alarcon C, Boland BB, Uchizono Y, et al. Pancreatic β-cell adaptive plasticity in obesity increases insulin production but adversely affects secretory function. Diabetes 2016;65:438–450

8. Erion KA, Berdan CA, Burritt NE, Corkey BE, Deeney JT. Chronic exposure to excess nutrients left-shifts the concentration dependence of glucose-stimulated insulin secretion in pancreatic β-cells. J Biol Chem 2015;290:16191–16201

9. Mehran AE, Templeman NM, Brigidi GS, et al. Hyperinsulinemia drives diet-induced obesity independently of brain insulin production. Cell Metab 2012;16:723–737
10. Attané C, Peyot M-L, Lussier R, et al. A beta cell ATGL-lipolysis/adipose tissue axis controls energy homeostasis and body weight via insulin secretion in mice. Diabetologia 2016;59:2654–2663
11. Cen J, Sargsyan E, Bergsten P. Fatty acids stimulate insulin secretion from human pancreatic islets at fasting glucose concentrations via mitochondria-dependent and -independent mechanisms. Nutr Metab (Lond) 2016;13:59
12. Boden G. Free fatty acids-the link between obesity and insulin resistance. Endocr Pract 2001;7:44–51
13. Maechler P, Wollheim CB. Mitochondrial function in normal and diabetic beta-cells. Nature 2001;414:807–812
14. Dobbins RL, Chester MW, Daniels MB, McGarry JD, Stein DT. Circulating fatty acids are essential for efficient glucose-stimulated insulin secretion after prolonged fasting in humans. Diabetes 1998;47:1613–1618
15. Wiederkehr A, Wollheim CB. Mitochondrial signals drive insulin secretion in the pancreatic β-cell. Mol Cell Endocrinol 2012;353:128–137
16. Prentki M, Matschinsky FM, Madiraju SRM. Metabolic signaling in fuel-induced insulin secretion. Cell Metab 2013;18:162–185
17. Kibbey RG, Pongratz RL, Romanelli AJ, Wollheim CB, Cline GW, Shulman GI. Mitochondrial GTP regulates glucose-stimulated insulin secretion. Cell Metab 2007;5:253–264
18. Wikstrom JD, Sereda SB, Stiles L, et al. A novel high-throughput assay for islet respiration reveals uncoupling of rodent and human islets [published correction appears in PLoS One 2013;8]. PLoS One 2012;7:e33023
19. Affourtit C, Brand MD. Stronger control of ATP/ADP by proton leak in pancreatic β-cells than skeletal muscle mitochondria. Biochem J 2006;393:151–159
20. Jastroch M, Divakaruni AS, Mookerjee S, Treberg JR, Brand MD. Mitochondrial proton and electron leaks. Essays Biochem 2010;47:53–67
21. Liesa M, Shirihai OS. Mitochondrial dynamics in the regulation of nutrient utilization and energy expenditure. Cell Metab 2013;17:491–506
22. Bernardi P, Di Lisa F. The mitochondrial permeability transition pore: molecular nature and role as a target in cardioprotection. J Mol Cell Cardiol 2015;78:100–106
23. Giorgio V, von Stockum S, Antoniel M, et al. Dimers of mitochondrial ATP synthase form the permeability transition pore. Proc Natl Acad Sci U S A 2013;110:5887–5892
24. Schinzel AC, Takeuchi O, Huang Z, et al. Cyclophilin D is a component of mitochondrial permeability transition and mediates neuronal cell death after focal cerebral ischemia. Proc Natl Acad Sci U S A 2005;102:12005–12010
25. Baines CP, Kaiser RA, Purcell NH, et al. Loss of cyclophilin D reveals a critical role for mitochondrial permeability transition in cell death. Nature 2005;434:658–662
26. Porter GA Jr., Beutner G. Cyclophilin D, somehow a master regulator of mitochondrial function. Biomolecules 2018;8:176
27. Kwong JQ, Molkentin JD. Physiological and pathological roles of the mitochondrial permeability transition pore in the heart. Cell Metab 2015;21:206–214
28. Taddeo EP, Laker RC, Breen DS, et al. Opening of the mitochondrial permeability transition pore links mitochondrial dysfunction to insulin resistance in skeletal muscle. Mol Metab 2013;3:124–134
29. Tavecchio M, Lisanti S, Bennett MJ, Languino LR, Altieri DC. Deletion of cyclophilin D impairs β-oxidation and promotes glucose metabolism. Sci Rep 2015;5:15981
30. Aharoni-Simon M, Shumiatcher R, Yeung A, et al. Bcl-2 regulates reactive oxygen species signaling and a redox-sensitive mitochondrial proton leak in mouse pancreatic β-cells. Endocrinology 2016;157:2270–2281
31. Lacy PE, Kostianovsky M. Method for the isolation of intact islets of Langerhans from the rat pancreas. Diabetes 1967;16:35–39
32. Taddeo EP, Stiles L, Sereda S, et al. Individual islet respirometry reveals functional diversity within the islet population of mice and human donors. Mol Metab 2018;16:150–159
33. Truchan NA, Brar HK, Gallagher SJ, Neuman JC, Kimple ME. A single-islet microplate assay to measure mouse and human islet insulin secretion. Islets 2015;7:e1076607
34. Assali EA, Shlomo D, Zeng J, et al. Nanoparticle-mediated lysosomal re-acidification restores mitochondrial turnover and function in β cells under lipotoxicity. FASEB J 2019;33:4154–4165
35. Taneera J, Lang S, Sharma A, et al. A systems genetics approach identifies genes and pathways for type 2 diabetes in human islets. Cell Metab 2012;16:122–134
36. Taneera J, Fadista J, Ahlqvist E, et al. Expression profiling of cell cycle genes in human pancreatic islets with and without type 2 diabetes. Mol Cell Endocrinol 2013;375:35–42
37. Kanatsuna N, Taneera J, Vaziri-Sani F, et al. Autoimmunity against INS-IGF2 protein expressed in human pancreatic islets. J Biol Chem 2013;288:29013–29023
38. Divakaruni AS, Brand MD. The regulation and physiology of mitochondrial proton leak. Physiology (Bethesda) 2011;26:192–205
39. Kenwood BM, Weaver JL, Bajwa A, et al. Identification of a novel mitochondrial uncoupler that does not depolarize the plasma membrane. Mol Metab 2013;3:114–123
40. Nolan CJ, Leahy JL, Delghingaro-Augusto V, et al. Beta cell compensation for insulin resistance in Zucker fatty rats: increased lipolysis and fatty acid signalling. Diabetologia 2006;49:2120–2130
41. Kristinsson H, Sargsyan E, Manell H, Smith DM, Göpel SO, Bergsten P. Basal hypersecretion of glucagon and insulin from palmitate-exposed human islets depends on FFAR1 but not decreased somatostatin secretion. Sci Rep 2017;7:4657
42. Kristinsson H, Bergsten P, Sargsyan E. Free fatty acid receptor 1 (FFAR1/GPR40) signaling affects insulin secretion by enhancing mitochondrial respiration during palmitate exposure. Biochim Biophys Acta 2015;1853:3248–3257
43. Samovski D, Kalderon B, Yehuda-Shnaidman E, Bar-Tana J. Gating of the mitochondrial permeability transition pore by long chain fatty acyl analogs in vivo. J Biol Chem 2010;285:6879–6890
44. Giorgio V, Burchell V, Schiavone M, et al. Ca^{2+} binding to F-ATP synthase β subunit triggers the mitochondrial permeability transition. EMBO Rep 2017;18:1065–1076
45. Waldmeier PC, Feldtrauer J-J, Qian T, Lemasters JJ. Inhibition of the mitochondrial permeability transition by the nonimmunosuppressive cyclosporin derivative NIM811. Mol Pharmacol 2002;62:22–29
46. Basso E, Fante L, Fowlkes J, Petronilli V, Forte MA, Bernardi P. Properties of the permeability transition pore in mitochondria devoid of Cyclophilin D. J Biol Chem 2005;280:18558–18561
47. Wikstrom JD, Katzman SM, Mohamed H, et al. β-cell mitochondria exhibit membrane potential heterogeneity that can be altered by stimulatory or toxic fuel levels. Diabetes 2007;56:2569–2578
48. Benninger RKP, Hodson DJ. New understanding of β-cell heterogeneity and in situ islet function. Diabetes 2018;67:537–547
49. Kilimnik G, Zhao B, Jo J, et al. Altered islet composition and disproportionate loss of large islets in patients with type 2 diabetes. PLoS One 2011;6:e27445
50. Newgard CB, An J, Bain JR, et al. A branched-chain amino acid-related metabolic signature that differentiates obese and lean humans and contributes to insulin resistance. Cell Metab 2009;9:311–326
51. Alemzadeh R, Fledelius C, Bodvarsdottir T, Sturis J. Attenuation of hyperinsulinemia by NN414, a SUR1/Kir6.2 selective K-adenosine triphosphate channel opener, improves glucose tolerance and lipid profile in obese Zucker rats. Metabolism 2004;53:441–447
52. Loves S, van Groningen L, Filius M, et al. Effects of diazoxide-mediated insulin suppression on glucose and lipid metabolism in nondiabetic obese men. J Clin Endocrinol Metab 2018;103:2346–2353
53. Velasquez-Mieyer PA, Cowan PA, Arheart KL, et al. Suppression of insulin secretion is associated with weight loss and altered macronutrient intake and preference in a subset of obese adults. Int J Obes Relat Metab Disord 2003;27:219–226

54. Joseph JW, Koshkin V, Saleh MC, et al. Free fatty acid-induced β-cell defects are dependent on uncoupling protein 2 expression. J Biol Chem 2004;279:51049–51056
55. Robson-Doucette CA, Sultan S, Allister EM, et al. β-cell uncoupling protein 2 regulates reactive oxygen species production, which influences both insulin and glucagon secretion. Diabetes 2011;60:2710–2719
56. Ly LD, Xu S, Choi SK, et al. Oxidative stress and calcium dysregulation by palmitate in type 2 diabetes. Exp Mol Med 2017;49:e291
57. Lablanche S, Cottet-Rousselle C, Lamarche F, et al. Protection of pancreatic INS-1 β-cells from glucose- and fructose-induced cell death by inhibiting mitochondrial permeability transition with cyclosporin A or metformin. Cell Death Dis 2011;2:e134
58. Fujimoto K, Chen Y, Polonsky KS, Dorn GW II. Targeting cyclophilin D and the mitochondrial permeability transition enhances beta-cell survival and prevents diabetes in Pdx1 deficiency. Proc Natl Acad Sci U S A 2010;107:10214–10219
59. Elrod JW, Molkentin JD. Physiologic functions of cyclophilin D and the mitochondrial permeability transition pore. Circ J 2013;77:1111–1122
60. Laker RC, Taddeo EP, Akhtar YN, Zhang M, Hoehn KL, Yan Z. The mitochondrial permeability transition pore regulator cyclophilin D exhibits tissue-specific control of metabolic homeostasis. PLoS One 2016;11:e0167910
61. Bertholet AM, Chouchani ET, Kazak L, et al. H^+ transport is an integral function of the mitochondrial ADP/ATP carrier. Nature 2019;571:515–520
62. Kampjut D, Sazanov LA. Structure and mechanism of mitochondrial proton-translocating transhydrogenase. Nature 2019;573:291–295
63. Briston T, Roberts M, Lewis S, et al. Mitochondrial permeability transition pore: sensitivity to opening and mechanistic dependence on substrate availability. Sci Rep 2017;7:10492
64. Jesinkey SR, Madiraju AK, Alves TC, et al. Mitochondrial GTP links nutrient sensing to β cell health, mitochondrial morphology, and insulin secretion independent of OxPhos. Cell Rep 2019;28:759–772.e10
65. Stark R, Pasquel F, Turcu A, et al. Phosphoenolpyruvate cycling via mitochondrial phosphoenolpyruvate carboxykinase links anaplerosis and mitochondrial GTP with insulin secretion. J Biol Chem 2009;284:26578–26590
66. Dhar-Chowdhury P, Harrell MD, Han SY, et al. The glycolytic enzymes, glyceraldehyde-3-phosphate dehydrogenase, triose-phosphate isomerase, and pyruvate kinase are components of the K(ATP) channel macromolecular complex and regulate its function. J Biol Chem 2005;280:38464–38470
67. Heit JJ, Apelqvist ÅA, Gu X, et al. Calcineurin/NFAT signalling regulates pancreatic β-cell growth and function. Nature 2006;443:345–349
68. Perkins ME, Wu TW, Le Blancq SM. Cyclosporin analogs inhibit in vitro growth of Cryptosporidium parvum. Antimicrob Agents Chemother 1998;42:843–848
69. Zhu S, Larkin D, Lu S, et al. Monitoring C-peptide storage and secretion in islet β-cells in vitro and in vivo. Diabetes 2016;65:699–709
70. Page MM, Johnson JD. Mild suppression of hyperinsulinemia to treat obesity and insulin resistance. Trends Endocrinol Metab 2018;29:389–399
71. Page MM, Skovsø S, Cen H, et al. Reducing insulin via conditional partial gene ablation in adults reverses diet-induced weight gain. FASEB J 2018;32:1196–1206
72. Patanè G, Piro S, Rabuazzo AM, Anello M, Vigneri R, Purrello F. Metformin restores insulin secretion altered by chronic exposure to free fatty acids or high glucose: a direct metformin effect on pancreatic β-cells. Diabetes 2000;49:735–740